International Journal of Nuclear Security

Volume 5 | Number 1

1-15-2019

Measurement and Analysis of the Extreme Physical Shock Environment Experienced by Crane-Mounted Radiation Detection Systems

Matthew Boyd
Texas A & M University - College Station

Jennifer Erchinger
Los Alamos National Laboratory

Craig M. Marianno
Texas A&M University

Gene Kallenbach
Sandia National Laboratory

International Journal of Nuclear Security, Vol.5, No.1, 2019

Measurement and Analysis of the Extreme Physical Shock Environment Experienced by Crane-Mounted Radiation Detection Systems

Boyd, M.[1], Erchinger, J.[2], Marianno, C.[1], Kallenbach, G.[3], Grypp, M.4
[1]Texas A&M Nuclear Engineering Department/Nuclear Security Science & Policy Institute
[2]Los Alamos National Laboratory
[3]Sandia National Laboratories
[4]US Navy

Abstract

At ports of entry, radiation detectors could be mounted on container gantry crane spreaders to monitor cargo containers entering and leaving the country. These detectors would have to withstand the extreme physical conditions experienced by these spreaders during normal operations. Physical shock data from the gable ends of a spreader were recorded during the loading and unloading of a cargo ship by two hard mounted PCB Piezotronics model 340A50 accelerometers and two Lansmont SAVER 9X30 units (with padding). The majority of large shocks were observed in the vertical direction. The Lansmont units recorded mean shocks of 22.215 $\pm$ 1.174 and 23.776 $\pm$ 1.140 g, while the PCB accelerometers recorded mean shocks of 31.608 $\pm$ 1.798 and 37.072 $\pm$ 2.015 g in this direction. Maximum shocks were as high as 118.854 g. A scatter plot of observed peak acceleration versus velocity change is presented to allow comparison with the damage boundary curve for any planned instrumentation for future systems. It is hoped that the results of this research will aid in the design of future crane-mounted systems.

I. Introduction

The SAFE Port Act requires that all containers entering the US through its 22 busiest ports be monitored for radiation **[*1*]**. Monitoring cargo for nuclear materials is essential for border security and non-proliferation efforts **[*2, 3*]**. To provide better radiation detection coverage on cargo containers, some companies have investigated the use of detection systems directly mounted to ship-to-shore container gantry cranes **[*2–4*]**. These spreaders weigh in excess of 15 tons and routinely collide with shipping containers and other objects at operating speeds during their day-to-day operations. Mounting radiation detectors on this type of crane would put the sensors in the closest possible proximity to cargo containers while minimizing background radiation contributions but these systems would undergo large amounts of physical stress during loading and off-loading operations **[*2*]**. Many radiation detectors are known to be susceptible to mechanical shock; NaI(Tl) scintillators, for example, are relatively brittle and fragile **[*5–7*]**.

Figure 1. Ship-to-Shore Container Gantry Crane, Port of Tacoma, Husky Terminal

Figure 1. Container Crane Spreader

The Spreader Bar Radiation Detector project was a joint effort of Sandia National Laboratories and Pacific Northwest National Laboratory, sponsored by the National Nuclear Security Agency's (NNSA) Office of Defense Nuclear Nonproliferation. Researchers in Texas A&M University's Nuclear Security Science and Policy Institute assisted in this work by collecting physical shock data using two different types of accelerometers at the Domestic Nuclear Detection Office's Test Track Facility at the Port of Tacoma's Husky Terminal (Figure 1) during normal operations. It is hoped that the results of this research will aid in the design of future crane-mounted systems.

System design for these conditions can be improved with direct observation of the physical shocks experienced by the spreader. Damage boundary theory is a testing protocol which determines which shock inputs will damage a product **[*8*]**. A combination of the acceleration level and velocity change, due to a shock, can cause product damage; however, there is a critical acceleration and critical velocity change, and both must be exceeded for damage to occur. A theoretical boundary damage curve can be seen in Figure 3. The shock environment of the spreader bar can be measured in advance for evaluation against the damage boundary curve for any proposed future instrumentation.

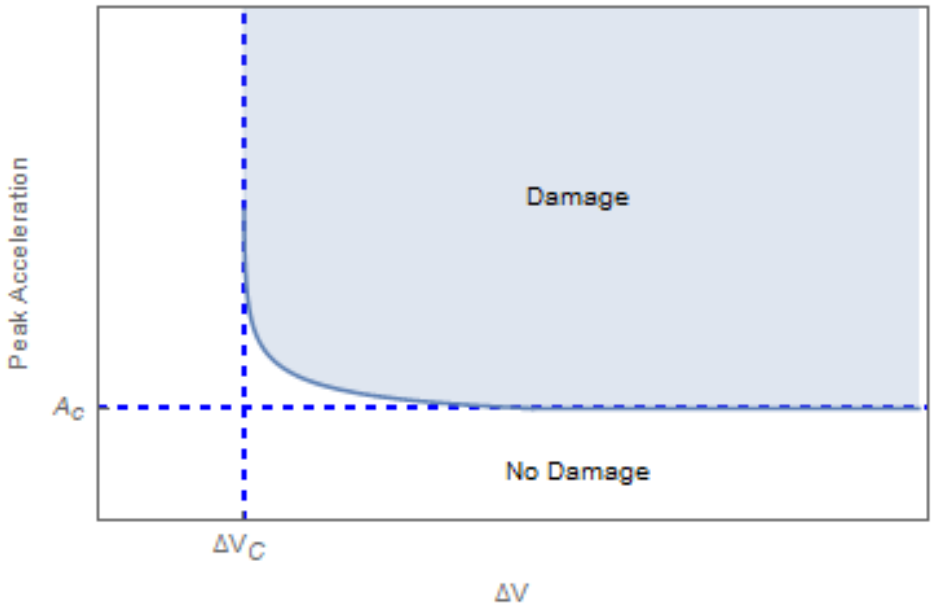

Figure 3. Theoretical damage boundary curve caused by a square waveform with arbitrary scaling. Product damage only occurs in the shaded region. A shock input above both the critical acceleration (A_C) and critical velocity change (ΔV_C) will cause damage.

II. Materials and Methods

To measure physical shock, two self-contained accelerometer units were fabricated at Sandia National Laboratory, each consisting of a Lansmont SAVER 9X30 accelerometer/data recorder and a PCB Piezotronics Model 340A50 tri-axial accelerometer within an aluminum housing. The PCB accelerometer was attached directly to the aluminum housing while the Lansmont accelerometer was braced in the case by high-density polyethylene foam (Figures 4 &5). The data from both accelerometers were stored by the Lansmont accelerometer. The Lansmont and PCB accelerometers were designated “internal” and “external” respectively, in accordance with their mounting location in the housing. The PCB accelerometers were previously calibrated by Sandia’s Primary Standards Lab and were in calibration during data collection. Calibration was checked on November 11, 2013 and found to be within specification. The Lansmont accelerometers were calibrated by the manufacturer. Sandia preformed a subsequent shock table test which showed very good agreement between the Lansmont accelerometer and the reference accelerometer.

Both units were attached to the gable ends of a spreader bar located at the Port of Tacoma’s Husky Terminal. The final placement of the units was decided by the Port of Tacoma; the resulting orientation aligned the x-axis perpendicular to the docks surface (i.e. up/down), the y-axis perpendicular to the ship (lateral movement of the crane), and the z-axis parallel to the length of the ship. One unit was mounted on

the landside of one gable end, and the other was mounted on the waterside portion of the opposite gable end, as shown in Figure 6.

Shock and vibration data were recorded over the unloading and loading of one ship. Data were stored internally, on separate channels for each axis of motion, and periodically transferred to a laptop. Both PCB accelerometers experienced mechanical and electrical faults, primarily on the Z axis channel; data from this channel were not included in analysis. Mechanically, mount loosening permitted the accelerometer to slide, resulting in large artificial accelerations. Electronically, the interface connectors repeatedly came loose, generating false signals with decay times of 1 to 10 seconds due to the open circuit input. The false data from these records were not included in analysis.

Figure 4. Lansmont SAVER 9X30 and Piezotronics Model 340A50

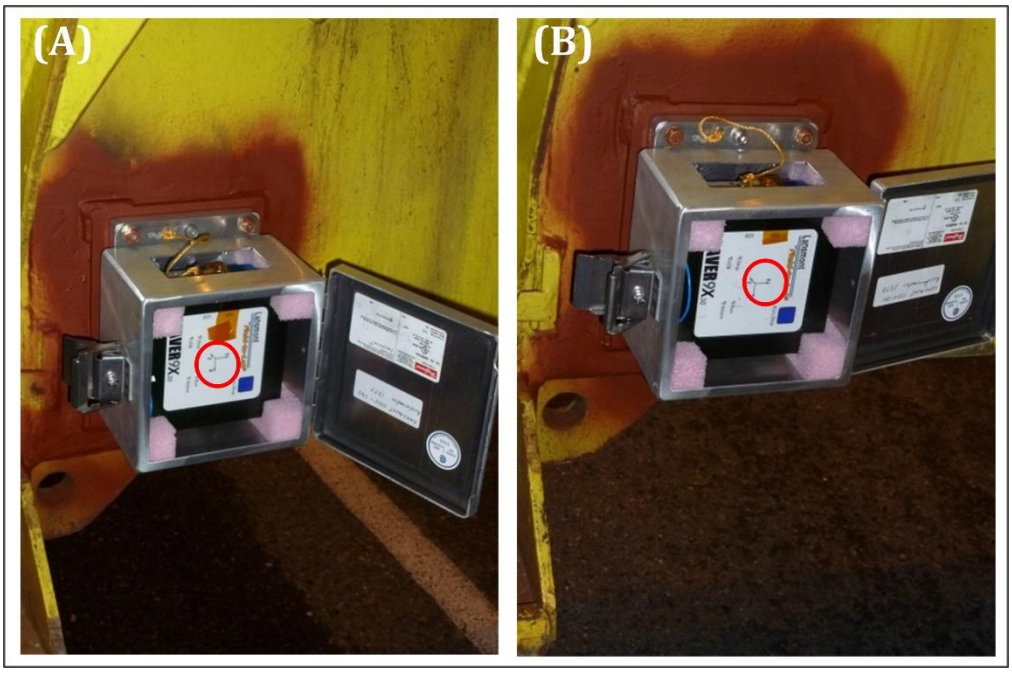

Figure 5. The land-side (A) and water-side (B) accelerometers shown in their housing, mounted on the bracket attached to the spreader bar. The axial orientations are circled in red.

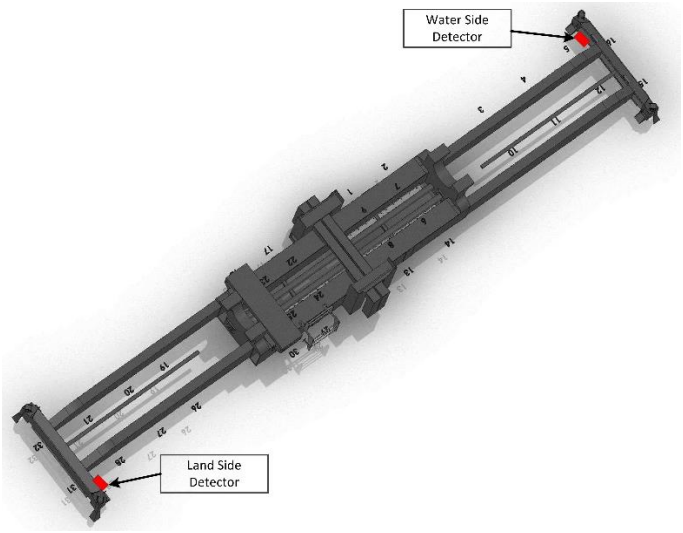

Figure 6. Rendering of the spreader showing placement of the landside and waterside detectors.

Data were transferred from the units to the laptop during regularly scheduled breaks in the loading and unloading of the ships. Data were collected beginning with the 8 AM shift on 19 March, 2012 and ending after the night shift, just before 8 AM on 21 March, 2012. Transfers to the laptop occurred just after 12:00 and 17:00 (lunch break and shift change) on 19 March and 20 March. The last transfer was completed after the ship was fully loaded at approximately 09:20 on 21 March, 2012. The data were exported as Comma Separated Values (CSV) files for further data analysis.

III. Results & Discussion

The data were obtained over two days of unloading and loading the ship. The accelerometers stored shock and vibration data internally, on separate channels for each axis of motion, until it was transferred to the

laptop with a USB connection. All units recorded severe physical shocks during the operation period. The z-axis shock data from the PCB accelerometers were neglected due to electronic and mechanical malfunctions. Additionally, it was observed that loose electronic connections created irregular spikes with decay times from 1 to 10 seconds. The false data from these records were removed from analysis. The shock and vibration data were plotted with respect to time using the SaverXware from Lansmont. A sample shock time history from the Landside unit on 20:29:34 19 March, 2012 (signal 131) is reproduced Figure 7.

The initial shock event occurs at ~40 ms. A large acceleration is detected on both the internal and external accelerometers. The primary shock is along the x axis, registering 38.48 g and 19.59 g on the external and internal accelerometers respectively. After ~20 ms and 60 ms, small aftershocks occur in alternating directions. Much smaller accelerations are simultaneously observed on the Y axis channels (peak 3.40 g internal and 7.28 g external) and the Z axis (peak 2.86 g internal). The largest accelerations were on the external (unpadded PCB) accelerometer. In general, the external accelerometer recorded sharp peak accelerations with shorter durations while the internal accelerometer recorded round lower peak accelerations with longer durations. This results in typically lower ΔV values for the external accelerometers. In this case, the internal accelerometer measured ΔV values of 57.91 and 5.39 [in s^{-1}] for the X and Y axes versus 41.28 and 3.05 [in s^{-1}] on the external. It is suspected that lower peak accelerations and rounder peak shape of the internal accelerometer is due to the padding presence of the small amount of polyethylene foam. The time history behavior of this shock is typical of the recorded data.

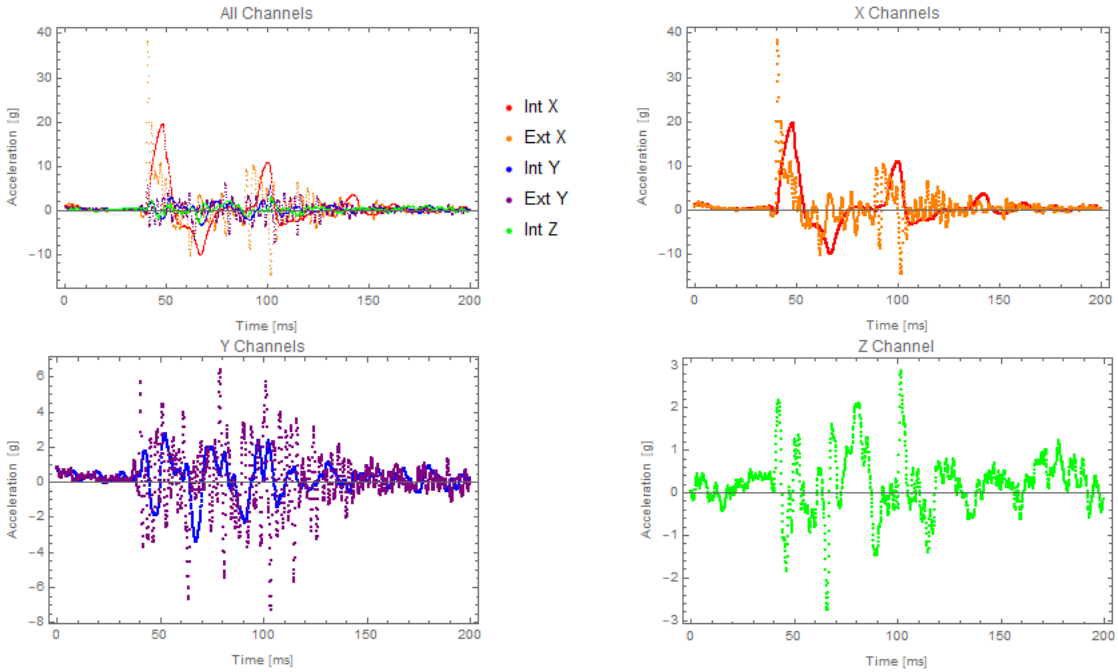

Figure 7: Sample shock time history from the Landside unit on 20:29:34 19 March, 20012 (signal 131). The data from all channels are plotted together and then separated and scaled by axis. The primary shock is along the X axis but smaller magnitude accelerations are also observed on the Y and Z axes.

A total of 476 shock events were recorded for the landside units while only 376 events were recorded for the waterside units. Due to the faulty electrical connections, the sample sizes for external accelerometers are smaller than the internal accelerometers. For all units, the data are right skewed due to the high outlying maximums. Histograms of the acceleration data from each unit are shown in Figure 8. A summary of the relevant statistics for the total data set is included in Table 1.

Several trends should be highlighted. First, the data are clearly non-Gaussian and right skewed with a large spread in the data across all channels. Additionally, in all units the majority of large shocks occurred along the X axis (vertical motion) resulting in the highest mean and maximum shocks in these channels. The mean shock values along the X axis are ~3 times those on the respective Y axis (perpendicular to the ship) for each detector. For the internal detectors, the mean X axis shock value is ~6 times the respective mean shock on the Z axis (parallel to ship). The maximum observed shock for each unit is along its X axis and is significantly larger than the maximum in any other direction. Both the internal detectors reported low maximum and mean values for shocks along the Z axis. During this study, this direction was relatively sheltered from mechanical shocks. If a proposed instrument has a weak axis that is more vulnerable to shock, such as the joint between the photo-multiplier tube and a scintillation crystal, it should be aligned in this direction to minimize the potential for damage.

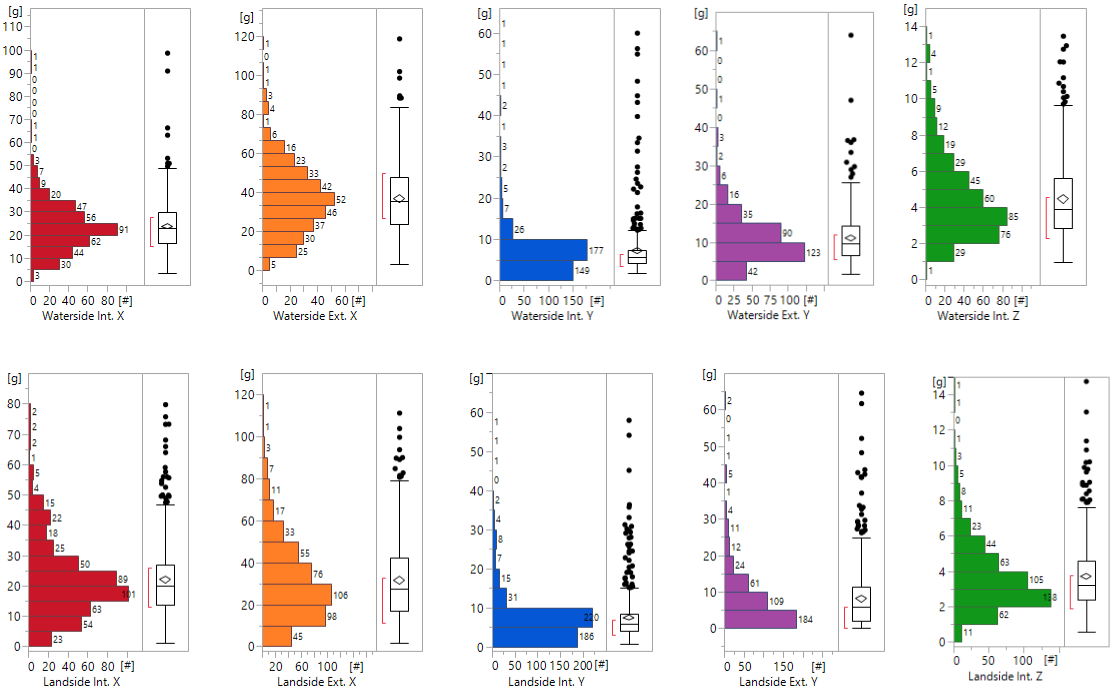

Figure 8. Histograms of the recorded shock data for each accelerometer by axis.

Table 1: Summary statistics of the recorded data.

Accelerometer Channel	Sample Size	Standard Deviation	Skew	Mean [g] 95% Confidence	Median [g]	Maximum [g]
Landside Int. X	476	13.071	1.268	22.215 ± 1.174	19.940	79.797
Landside Int. Y	476	6.600	3.516	7.507 ± 0.593	5.908	57.941
Landside Int. Z	476	1.977	1.558	3.711 ± 0.178	3.204	14.740
Landside Ext. X	453	19.523	1.080	31.608 ± 1.798	27.246	111.231
Landside Ext. Y	415	9.449	2.416	8.255 ± 0.912	5.817	64.661
Waterside Int. X	376	11.279	1.744	23.776 ± 1.140	22.991	98.749
Waterside Int. Y	376	7.375	4.403	7.375 ± 0.745	5.618	60.059
Waterside Int. Z	376	2.267	1.205	4.476 ± 0.229	3.915	13.477
Waterside Ext. X	326	15.566	0.782	37.072 ± 2.015	35.538	118.854
Waterside Ext. Y	319	7.128	2.521	11.259 ± 0.782	9.656	64.086

It is noted that the external accelerometers recorded larger mean and maximum shocks than the internal detectors with a greater spread in the data. It is unclear if this variance is due to differences in function between the accelerometer models used or a result of the padding used on the internal accelerometers. Additionally, the landside accelerometers show slightly more variance than the waterside ones. Despite this, the waterside units reported the largest maximum shock for both the internal and external accelerometers. However, peak acceleration alone will not cause damage; a sufficient velocity change, from a shock, must also occur. There is a critical acceleration and critical velocity change, and both must be exceeded for damage to result. The critical acceleration and critical velocity change required to cause damage will be instrument dependent. For example, Saint Gobian rates its 2" X 18"NaI(Tl) detectors for maximum shocks of 5g's at 10 ms in any direction while its PolyScin® NaI(Tl) are rated for 200g's at 5 ms. To aid in future instrumentation selection, a cumulative scatterplot of the observed peak accelerations and corresponding ΔV is provided in Figure 9, along with scaled plots of each axis for comparison with product damage boundary curves.

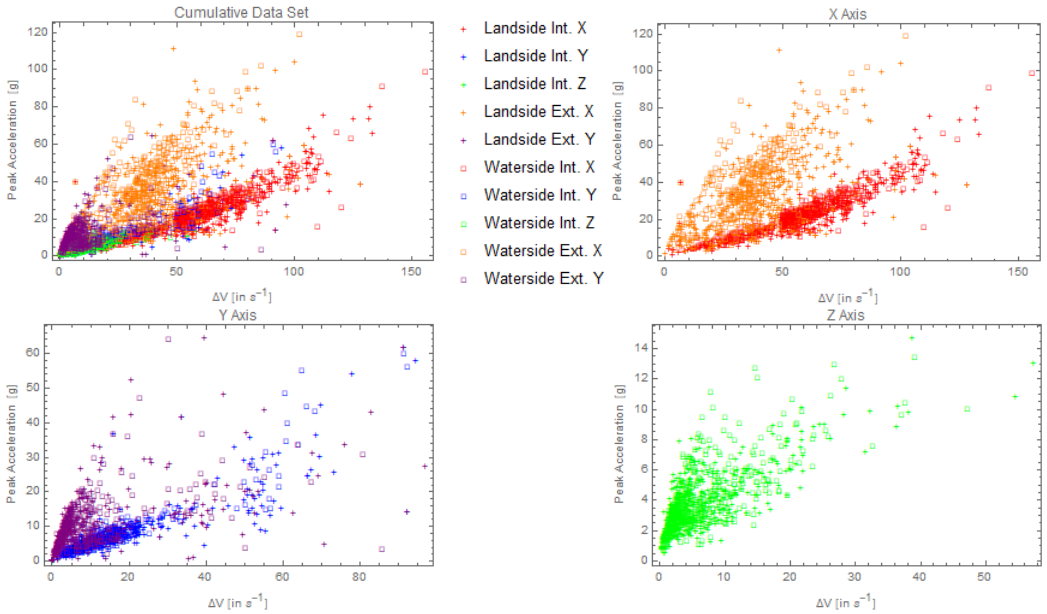

Figure 9: Peak acceleration [g] versus velocity change [in s^{-1}]. Landside values are plotted as + ; Waterside values as □. A cumulative data set and scaled plot for each axis is presented.

A few key observations can be made from these plots. First, the highest accelerations and ΔV values are observed along the X axis, while the lowest are observed along the Z axis. When designing a system, the weakest axis should be aligned parallel to the length of dock to minimize the possibility of damage. Additionally, there is not a significant difference between the maximum events for the landside and waterside units, though there is a noticeable difference between the external and internal accelerometers. The unpadded external accelerometers show higher shocks with lower velocity changes, while the padded internal accelerometers show lower peak shocks with larger velocity changes. This is believed to be due to small amounts of polyethylene padding present around the internal units, as the function of padding is to translate high acceleration events outside the packaging to lower acceleration events for the internal object. Any system designed to operate in these environments must be able to limit input accelerations below critical accelerations levels. Low Z padding is the suggested method to minimize attenuation and preserve detector sensitivity.

IV. Conclusions

This work shows that detection systems mounted on the gable ends of a spreader will operate in an extreme shock environment. During loading and unloading shifts, crane operators are mainly concerned with working as quickly as possible and will not slow down for fragile systems. The largest peak accelerations and most potentially damaging events were observed along the vertical axis. The slightly padded Lansmont units recorded mean shocks of 22.215 ± 1.174 and 23.776 ± 1.140 g's with maximum shocks of 79.797 and 98.749 g's in this direction; the hard-mounted PCB accelerometers recorded mean shocks of 31.608 ± 1.798 and 37.072 ± 2.015 g's with maximum shocks of 111.231 and 118.854 g's. The lowest peak accelerations and least potentially damaging events were observed parallel to the dock. A scatterplot of the observed peak accelerations and corresponding ΔV in the environment is presented to aid instrumentation selection for future systems. Systems should be designed to withstand maximum shock inputs of over 120 g's in the vertical direction, over 60g's in the lateral direction of the crane, and 20 g's parallel to the dock, or sufficiently cushioned to lower received internal accelerations to

acceptable levels for a given instrument. Low-Z padding is suggested to stabilize the detector and protect it from large shocks while not overly inhibiting the detection mechanisms.

V. Acknowledgements

We would like to thank the National Nuclear Security Agency's Office of Defense Nuclear Nonproliferation for their support of research and development in the nuclear security field.

We would like to thank the Port of Tacoma and Husky Terminal for their support and cooperation in the collection of this data.

We would like to thank Gene Kallenbach and the Nuclear Monitoring and Transparency Department at Sandia National Laboratories for including us in this project.

VI. Works Cited

1. D. Lungren, *H.R.4954 - 109th Congress (2005-2006): SAFE Port Act* (2006; https://www.congress.gov/bill/109th-congress/house-bill/4954).

2. M. D. Grypp, C. M. Marianno, J. W. Poston, G. C. Hearn, *Design of a Spreader Bar Crane-Mounted Gamma-Ray Radiation Detection System* (2014), vol. 743.

3. J. H. Ely, E. D. Ashbaker, M. T. Batdorf, J. E. Baciak, W. K. Hensley, K. D. Jarman, S. M. Robinson, G. A. Sandness, J. E. Schweppe, "Spreader-Bar Radiation Detection System Enhancements: A Modeling and Simulation Study" (PNNL-21948, 1088649, Pacific Northwest National Laboratory, Richland, WA, 2012), , doi:10.2172/1088649.

4. R. H. Redus, M. Alioto, D. Sperry, T. Pantazis, VeriTainer Radiation Detector for Intermodal Shipping Containers. *Nucl. Instrum. Methods Phys. Res. Sect. Accel. Spectrometers Detect. Assoc. Equip.* **579**, 384–387 (2007).

5. K. O. Findley, J. Johnson, D. F. Bahr, F. P. Doty, J. Frey, (2007; https://doi.org/10.1117/12.740822), vol. 6707, pp. 670706-6707–12.

6. K. Forrest, C. Haehner, T. Heslin, M. Magida, J. Uber, S. Freiman, R. Polvani, Engineering and Design Properties of Thallium-Doped Sodium Iodide and Selected Properties of Sodium-Doped Cesium Iodide. *NASA Ref. Publ. 1131*, 76 (1984).

7. G. F. Knoll, *Radiation Detection and Measurement* (John Wiley, Hoboken, N.J, 4th ed., 2010).

8. R. E. Newton, "Fragility Assessment Theory and Test Procedure" (Naval Postgraduate School, Monterey, CA, 1968), (available at http://hdl.handle.net/10945/27486).